

Single-pulse multiphoton polymerization of complex structures using a digital multimirror device

Benjamin Mills,^{1,*} James A Grant-Jacob,¹ Matthias Feinaeugle,¹
and Robert W Eason¹

¹*Optoelectronics Research Centre, University of Southampton, Southampton, SO17 1BJ, UK*
bm602@orc.soton.ac.uk

Abstract: We present a rapid technique for the patterning of complex structures with $\sim 2\mu\text{m}$ resolution via multiphoton polymerization, through use of a single ultrashort pulse in combination with the spatial intensity modulation possible from a digital multimirror device. Sub-micron features have been achieved through the use of ten consecutive pulses.

©2013 Optical Society of America

OCIS codes: (180.4315) Nonlinear microscopy; (190.4180) Multiphoton processes; (220.4000) Microstructure fabrication; (220.4610) Optical fabrication.

References and links

1. B. Mills, M. Feinaeugle, C. L. Sones, N. Rizvi, and R. W. Eason, "Sub-micron-scale femtosecond laser ablation using a digital micromirror device," *J. Micromech. Microeng.* **23**(3), 035005 (2013).
2. J. P. Rice, J. E. Neira, M. Kehoe, and R. Swanson, "DMD diffraction measurements to support design of projectors for test and evaluation of multispectral and hyperspectral imaging sensors," *Proc. SPIE* **7210**, 72100D, 72100D-9 (2009), doi:10.1117/12.808990.
3. D. Dudley, W. M. Duncan, and J. Slaughter, "Emerging digital micromirror device (DMD) applications," *Proc. SPIE* **4985**, 14–25 (2003), doi:10.1117/12.480761.
4. I. Ortega, A. J. Ryan, P. Deshpande, S. MacNeil, and F. Claeysens, "Combined microfabrication and electrospinning to produce 3-D architectures for corneal repair," *Acta Biomater.* **9**(3), 5511–5520 (2013).
5. R. E. Williams, (2002) US Patent 6413251.
6. M. Malinauskas, A. Zukauskas, G. Bickaускаite, R. Gadonas, and S. Juodkazis, "Mechanisms of three-dimensional structuring of photo-polymers by tightly focussed femtosecond laser pulses," *Opt. Express* **18**(10), 10209–10221 (2010).
7. G. von Freymann, A. Ledermann, M. Thiel, I. Staude, S. Essig, K. Busch, and M. Wegener, "Three-Dimensional Nanostructures for Photonics," *Adv. Funct. Mater.* **20**(7), 1038–1052 (2010).
8. M. Farsari and B. N. Chichkov, "Two-photon fabrication," *Nat. Photonics* **3**(8), 450–452 (2009).
9. J. Serbin, A. Ovsianikov, and B. Chichkov, "Fabrication of woodpile structures by two-photon polymerization and investigation of their optical properties," *Opt. Express* **12**(21), 5221–5228 (2004).
10. L. Erdmann, A. Deparnay, G. Maschke, M. Langle, and R. Brunner, "MOEMS-based lithography for the fabrication of micro-optical components," *J. Micro Nanolith.* **4**(4), 041601 (2005).
11. J.-W. Choi, M. D. Irwin, and R. B. Wicker, "DMD-based 3D micro-manufacturing," *Proc. SPIE* **7596**, 75960H, 75960H-11 (2010), doi:10.1117/12.846287.
12. R. Nielson, B. Kaehr, and J. B. Shear, "Microreplication and Design of Biological Architectures Using Dynamic-Mask Multiphoton Lithography," *Small* **5**(1), 120–125 (2009).
13. K. Obata, J. Koch, U. Hinze, and B. N. Chichkov, "Multi-focus two-photon polymerization technique based on individually controlled phase modulation," *Opt. Express* **18**(16), 17193–17200 (2010).
14. H. Misawa, T. Kondo, S. Juodkazis, V. Mizeikis, and S. Matsuo, "Holographic lithography of periodic two- and three-dimensional microstructures in photoresist SU-8," *Opt. Express* **14**(17), 7943–7953 (2006).
15. M. Tang, Z. C. Chen, Z. Q. Huang, Y. S. Choo, and M. H. Hong, "Maskless multiple-beam laser lithography for large-area nanostructure/microstructure fabrication," *Appl. Opt.* **50**(35), 6536–6542 (2011).
16. E. Stankevicius, T. Gertus, M. Rutkauskas, M. Gedvilas, G. Raciukaitis, R. Gadonas, V. Smilgevicius, and M. Malinauskas, "Fabrication of micro-tube arrays in photopolymer SZ2080 by using three different methods of a direct laser polymerization technique," *J. Micromech. Microeng.* **22**(6), 065022 (2012).
17. H. Lin, B. Jia, and M. Gu, "Dynamic generation of Debye diffraction-limited multifocal arrays for direct laser printing nanofabrication," *Opt. Lett.* **36**(3), 406–408 (2011).
18. M. Farsari, S. Huang, P. Birch, F. Claret-Tournier, R. Young, D. Budgett, C. Bradfield, and C. Chatwin, "Microfabrication by use of a spatial light modulator in the ultraviolet: Experimental results," *Opt. Lett.* **24**(8), 549–550 (1999).

19. Y.-C. Li, L.-C. Cheng, C.-Y. Chang, C.-H. Lien, P. J. Campagnola, and S.-J. Chen, "Fast multiphoton microfabrication of freeform polymer microstructures by spatiotemporal focusing and patterned excitation," *Opt. Express* **20**(17), 19030–19038 (2012).
 20. Texas Instruments, (2012) <http://www.ti.com/lit/ds/symlink/dlp3000.pdf> (last accessed 5/4/2013)
 21. A. Ovsianikov, J. Viertl, B. Chichkov, M. Oubaha, B. MacCraith, I. Sakellari, A. Giakoumaki, D. Gray, M. Vamvakaki, M. Farsari, and C. Fotakis, "Ultra-Low Shrinkage Hybrid Photosensitive Material for Two-Photon Polymerization Microfabrication," *ACS Nano* **2**(11), 2257–2262 (2008).
 22. S. Maruo, T. Hasegawa, and N. Yoshimura, "Single-anchor support and supercritical CO₂ drying enable high-precision microfabrication of three-dimensional structures," *Opt. Express* **17**(23), 20945–20951 (2009).
-

1. Introduction

There is considerable interest in the use of digital multimirror devices (DMDs) for laser-based machining, as they can offer both rapid and high-resolution fabrication [1]. For micron-scale fabrication, laser machining via DMDs is proposed as an alternative approach to existing focused-ion-beam and electron-beam lithography-based techniques which, although offering significantly higher resolutions, are both based on serial processing, and hence are intrinsically much slower fabrication tools. Due to their low-cost and high switching speeds, DMDs are rapidly becoming an attractive approach for applications in the photonics and medical sciences [2–5].

In this paper, we demonstrate the capability for single-pulse DMD-based multiphoton polymerization (MPP). MPP is a technique that uses focused, high-intensity laser pulses to produce a highly-localized chemical reaction inside a target resist [6], which results in the polymerization of the irradiated region. Since MPP is a nonlinear threshold process, the polymerized region can be set to be some fraction of the size of the laser focus hence enabling sub-100nm (and sub-diffraction-limited) writing resolution [7–9]. In general, to build up a 3D structure, the sample is scanned using high-precision actuators, relative to the laser focus, thus building up a network of overlapping voxels (3D pixels). Whilst this approach can produce extremely high-resolution structures, a major disadvantage is the time required for fabrication, due to the small interaction volume, the serial nature of the processing and the requirement of multiple laser pulses per voxel. Research into the parallelization of this fabrication technique through methods such as DMD-based lithography [10–12], spatial light modulators to produce multiple independent foci [13], diffractive beam elements to produce multiple writing spots [14,15], optical elements to make structured light [16], and phase retrieval algorithms and spatial light modulators to produce photonic crystals [17] are clearly of interest to those involved in MPP and laser direct-write techniques. In this work, we demonstrate single-pulse fabrication of complex structures using a DMD-based approach.

Through the use of a DMD to spatially shape the intensity profile of the incident laser pulse, we have been able to demonstrate a significant increase in writing speed, at the price of only a small loss in writing resolution. DMD-based MPP generally has the advantage over other spatial-light-modulator based approaches [18], in both cost and electronic switching speed. Here, we continue the progress shown by Li *et al.* [19] (which shows fabrication times on the order of seconds to minutes, and resolution on the order of 10 microns) and we present results obtained via both single ultrashort pulses and 10 pulses (with <1 μ m features).

2. Experimental Setup

The Texas Instruments DMD (DLP 3000) [20] that was used in this work is a device that has an array of 608 by 684 square mirrors, each of width:7.6 μ m, arranged in a diagonal square lattice (i.e. a checkerboard pattern that is rotated by 45°), where the centre-to-centre diagonal distance is 7.64 μ m. The horizontal and vertical centre-to-centre distance of adjacent mirrors is 10.8 μ m. The individual mirrors have two states of operation ('on' or 'off'), which describe the angular orientation of each DMD mirror (+ 12° or –12°) relative to the surface of the device. When used with incoherent light, these mirror orientations are used to control the RGB level of light that is projected by the device. Here, we have used these orientations to control which regions of a sample are illuminated, via a static black ('off') and white ('on') image. The behavior of the DMD is very different for coherent light, however, as the periodic

mirror array acts as a diffraction grating. The number of diffraction peaks and their angles relative to the DMD surface depends on the angle of the incident light, the wavelength and the grating period, where the optimal DMD angle can be determined through use of a variant of the Bragg equation, $\sin(\vartheta_i) - \sin(\vartheta_m) = m\lambda/d$ where ϑ_i and ϑ_m are the incident and reflected angles, d is the mirror period, λ is the wavelength and m is the diffraction order. The experimental setup used is shown in Fig. 1.

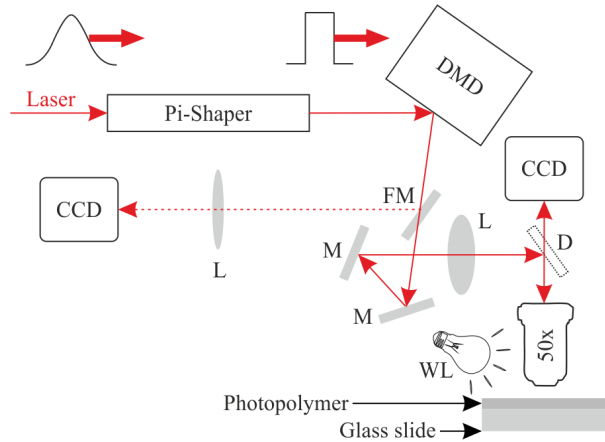


Fig. 1. Schematic of the experimental setup.

Ultrashort pulses from a 1mJ, 1kHz repetition rate, Ti:sapphire amplifier (150fs, 800nm) were spatially homogenized (via a π -shaper model 6_6, www.pishaper.com) and illuminated the DMD where they were diffracted into multiple orders. By setting the angle of the DMD so that the direction of the incident light was set to $\sim 57^\circ$ from the DMD surface normal (hence taking advantage of the blaze angle of the grating, which corresponded to the $\pm 12^\circ$ mirror angle), 75% of the diffracted light appeared within a single diffraction order. In this case, the $m = 4$ diffraction peak was used, which had a diffracted angle of 33° from the DMD surface normal (subsequent work has utilized an incident angle of 27° corresponding to $m = 3$ and a diffracted angle of 0°). The total reflectivity of the device was found to be 59%, and hence 44% of all light incident on the DMD could be used for polymerization within this $m = 4$ diffracted order. Additional optical losses resulted from the gaps between the mirrors and the inherent loss at each mirror surface (0.88 reflectivity at 800nm). The chosen diffracted order was then captured by a collimating lens and imaged using a 50x objective into the target polymer. Diffracted light was then directed along one of two beam paths, via a flip mirror (FM). Path 1 was a diagnostic line where the pulses were imaged via a lens (L) on to a CCD. Path 2 was used for sample fabrication, where the pulses were reflected off two mirrors (M), collimated using a lens (L), reflected off the front surface of a dichroic mirror (D) and then imaged on to the sample via a 50x (NA = 0.55) objective. The resolution of this DMD-based fabrication process was limited by the wavelength (via the diffraction limit) and hence the magnification strength of the objective had little influence on the resolution. We therefore chose to use a 50x objective (rather than a 100x or higher) in order to increase the field-of-view and hence pattern larger areas for each single pulse. The white light (WL) was used to enable real-time viewing of the fabrication process, and the sample was positioned on a 3-axis stage ($<1\mu\text{m}$ positional accuracy with total travel of 20mm). Monochrome bitmap images were imported onto the DMD via a USB connection and then displayed on the multimirror array. The photopolymer used here was a mixture of 8:2 MAPTMS:ZPO mole, 1:1 ZPO:methacrylic acid mole, with the photoinitiator a 1% mole to MAPTMS [21]. The structures presented here are, in general, $\sim 10\mu\text{m}$ thick, corresponding to the thickness of the photopolymer that was spin-coated onto the glass slide.

3. Single Structures

Figure 2 shows the effect of direct and complementary images – by inverting the black/white balance on the DMD images, the complementary structure can be fabricated. The figure shows SEM images of structures fabricated using ten laser pulses, corresponding to a total fabrication time of 10ms (as a 1kHz repetition rate laser was used here). In each case, the inset shows the binary pattern (black/white) that was displayed on the DMD, where white corresponds to laser light, and black to no laser light. The modulated edges on the left and right sides on some of the fabricated structures are believed to be a consequence of clipping at the DMD edge. This effect can be removed by avoiding the use of the mirrors at the boundary edges. Due to the magnification inherent in the imaging system (each DMD mirror geometrically scaled to $\sim 120\text{nm}$ in the sample), DMD patterns that corresponding to sub-micron features could be made. As shown in Fig. 2, via 10 pulses, we were able to fabricate complex structures with $<1\mu\text{m}$ features. As the experimental system was not a perfect imaging system (i.e. not all of the high spatial frequencies on the DMD were captured by the imaging lens), thin features on the DMD were imaged inside the photoresist with a lower than expected intensity [1]. Therefore, for the pattern in Fig. 2, there was not sufficient energy in a single to fabricate the structure. We believe that a higher-intensity pulse would enable single pulse fabrication of this pattern. By using a pattern which consists of wider features, single-shot fabrication has been demonstrated, as shown in Fig. 3, which demonstrates the achievable consistency with regard to feature size and edge-quality. The features in the center of the letters ‘O’ and ‘R’ were occasionally misplaced, likely as a result of the coalescing of features caused by the surface tension of the solvent that was used for development of the photopolymer, an effect that can be minimized through use of a critical point dryer [22].

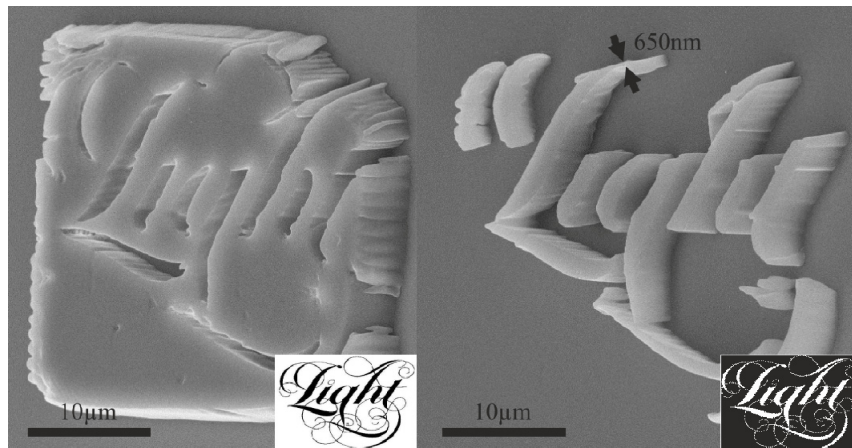


Fig. 2. SEM images of samples fabricated using 10 pulses, with insets showing the images loaded onto the DMD, viewed at 45 degrees.

In conventional MPP, the optimal resolution (the minimum distance between resolvable features) and minimum feature sizes (the smallest individual feature) are closely linked, as the fabrication process is point-by-point, and generally both can be $\sim 100\text{nm}$. However, in the DMD-based approach that is presented here, large areas of photoresist are processed at once, and hence the optimal resolution is $\sim \lambda$ (due to the diffraction limit). Due to the difficulty in capturing all spatial frequencies from the DMD, the intensity profile that was imaged inside the photoresist was not an ideal square-wave (but rather only closely resembled one), therefore, there was some intensity dependence on the size of individual features, and hence individual features fabricated using this approach can be $< \lambda$.

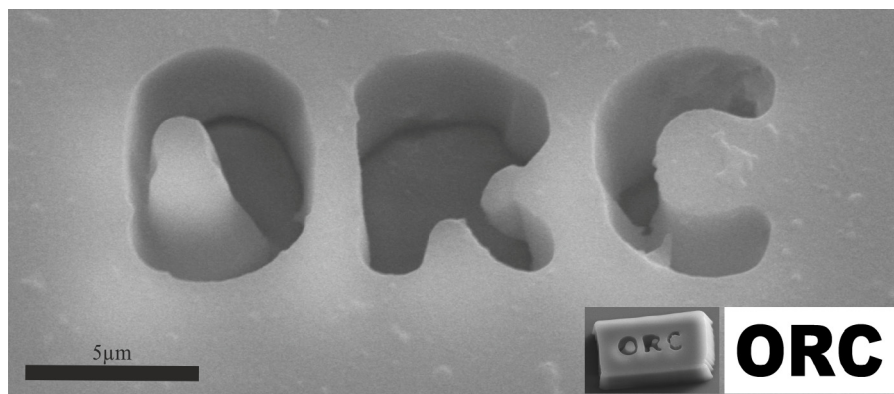


Fig. 3. SEM image of structure fabricated using a single pulse. Insets show SEM of a structure fabricated under the same conditions and DMD pattern used.

There is a significant difference between the 3D structures formed via the DMD-based approach presented here and the conventional point-by-point MPP. With the latter, the individual voxels that are joined together to produce a 3D structure, have a height (along the axis of the beam) that can be $\sim 200\text{nm}$, hence allowing a new different ‘layer’ to be added every $\sim 200\text{nm}$. With the approach presented here, the height of the polymerized region depends on the DMD pattern that is used, but has generally been observed to be $>10\mu\text{m}$, and so the point-by-point approach of producing multiple layers is not appropriate. Rather than a simple voxel, the DMD-based approach can produce a complex 2D intensity spatial profile, which may be considerably different for positions away from the image plane. Therefore, the 3D structure that can be fabricated will correspond to the positions where the diffracted beam intensity is above the polymerization threshold. This effect is demonstrated in Fig. 4, where a 3D structure fabricated using a single pulse, in a $\sim 100\mu\text{m}$ thick resist, is shown. Whilst the top-down view closely matches the DMD pattern (shown in the inset), away from the image plane (which was set to be the top of the object) the structure has a significantly different spatial profile. In order to produce a useful 3D structure using this DMD-based approach, the 3D propagation effects must therefore be taken into account. Whilst this DMD-based approach can only therefore make a limited number of 3D profiles, it does have the advantage that it may still only require a single pulse for fabrication.

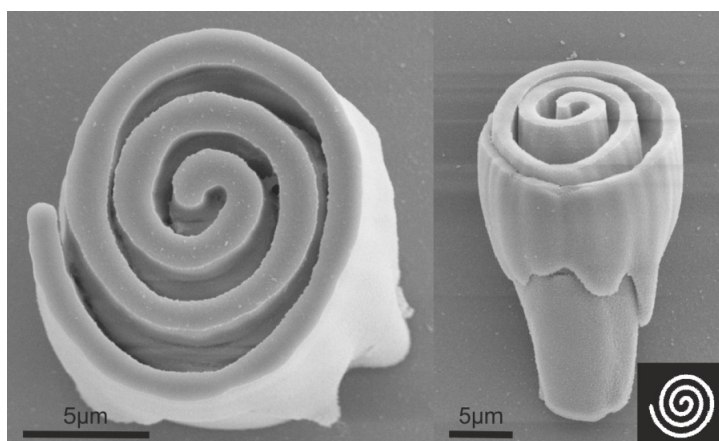


Fig. 4. SEM images of a 3D spiral pattern fabricated in a single pulse, in a $\sim 100\mu\text{m}$ thick resist, with inset showing the DMD pattern used.

4. Contiguous Structures

If the separation distances and DMD pattern are appropriately chosen, then the individual structures can be made contiguous. Figure 5 shows an example of what can be achieved, where each adjacent image was formed using a single pulse. The dotted lines represent the approximate size and position of the individual objects (where each object is fabricated under identical conditions to that demonstrated in Fig. 3), in order to elucidate the level of overlap used during fabrication. The slight angular disparity of the text with respect to the stage movement axes is believed to be a slight misalignment of the vertical axis of the DMD surface. On the assumption that 1000 structures with width of $30\mu\text{m}$ can be fabricated in 1 second (based on the 1kHz laser repetition rate), a coverage of 1mm^2 could, in theory, be fabricated within a timescale of order seconds. However, in practice, it is likely that the stage movement would not be accurate enough when operating at this required speed. In practice, for our experimental setup, coverage of 1mm^2 can be achieved within two minutes, and hence 1cm^2 on the order of a few hours. This, coupled with computer-automated control of the DMD pattern (i.e. changing the pattern between each laser pulse), will enable the fabrication of contiguous arbitrarily-shaped 2D devices.

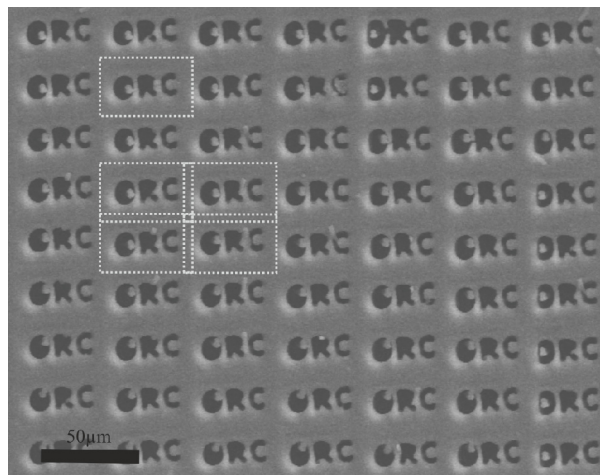


Fig. 5. Part of a large contiguous array of objects that have been fabricated using a single shot, stitched together by careful selection of object separation.

5. Conclusion

In conclusion, we have presented a single-pulse technique for the fabrication of complex structures via multiphoton polymerization. In addition, we have been able to fabricate these structures in arrays of $\sim\text{mm}$ size within a time scale of order minutes, representing orders of magnitude improvement in fabrication speed, with only a small loss in writing resolution. We anticipate that this work will lead to applications in fields including optics, nanomaterials and medical micro-devices. Future work will concentrate on the optimal resolution achievable when fabricating using single pulses.

Acknowledgments

The authors are grateful to the EU Seventh Framework Programme for funding under the grant, e-LIFT (247868-FP7-ICT-2009-4), and to the Engineering and Physical Sciences Research Council (EPSRC) under grant no EP/J008052/1. The authors would like to thank Dr. Maria Farsari for useful discussions and assistance with the preparation of the photopolymer.